FUNCTIONALS WITH $P(X)$-GROWTH IN IMAGE RESTORATION

YUNMEI CHEN*, STACEY LEVINE†, AND MURALI RAO‡

Abstract. We study a functional of $p(x)$ growth ($p(x) \geq 1$) which provides a model for image denoising, enhancement, and restoration. The diffusion resulting from the proposed model is a combination of Total Variation based regularization and Gaussian smoothing. The existence, uniqueness, and long-time behavior of the proposed model are established. Experimental results illustrate the effectiveness of the model in image restoration.

Key words. image restoration, p(x)-growth, BV-space, Dirichlet boundary condition

AMS subject classifications. 49J40, 35K65

1. Introduction.

1.1. Background. In this paper we propose a new model for image restoration. The version of this problem we address is to recover an image, u, from an observed, noisy image, I, where the two are related by $I = u + noise$. The proposed model incorporates the strengths of the various types of diffusion arising from the minimization problem

$$\min \int_\Omega |Du|^p + \frac{\lambda}{2}(u - I)^2 \tag{1.1}$$

for $1 \leq p \leq 2$ ($\lambda \geq 0$ and Ω is an open, bounded subset of $\mathbb{R}^n$ with Lipshitz boundary). Specifically, we exploit the benefits of isotropic diffusion ($p = 2$), total variation based diffusion ($p = 1$), and more general anisotropic diffusion ($1 < p < 2$).

Total Variation Minimization, $p = 1$:

Total Variation (TV) based regularization, $p = 1$, as first proposed by Rudin, Osher and Fatemi [18] does an excellent job at preserving edges while reconstructing images. Mathematically this is reasonable, since it is natural to study solutions of this problem in the space of functions of bounded variation, $BV(\Omega)$, allowing for discontinuities which are necessary for edge reconstruction. This phenomenon can also be explained physically, since the resulting diffusion is strictly orthogonal to the gradient of the image. The TV model has been studied extensively (see [1, 4], et.al) and has proved to be an invaluable tool for preserving edges in image restoration problem.

Given the success of TV-based diffusion, various modifications have been introduced. For instance, Chan and Strong [19] proposed the Adaptive Total Variation model

$$\min \int_\Omega \alpha(x)|\nabla u|$$

in which they introduce a control factor, $\alpha(x)$, which slows the diffusion at likely edges. This controls the *speed* of the diffusion and has demonstrated good results as it aids in noise reduction. It is also good at reconstructing edges, since the *type* of diffusion (strictly orthogonal to the image gradient) is the same as that of the original TV model.

TV-based denoising favors solutions that are piecewise constant. This sometimes causes a *staircasing* effect [2, 4, 15] in which noisy smooth regions are processed into piecewise constant regions (see figure 5.1), a phenomenon long observed in the literature, e.g. [8, 15, 17, 20, 21]. Not only do 'blocky' solutions fail to satisfy the ubiquitous 'eyeball norm', but they can also develop 'false edges' which can mislead a human or computer into identifying erroneous features not present in the true image.

*Department of Mathematics, P.O. Box 118505, University of Florida, Gainesville, FL, 32611 (yun@math.ufl.edu).
†Department of Mathematics and Computer Science, Duquesne University, Pittsburgh, PA, 15282 (sel@mathcs.duq.edu).
‡Department of Mathematics, P.O. Box 118505, University of Florida, Gainesville, FL, 32611 (rao@math.ufl.edu).

Minimization Problem (1.1) **with** $1 < p \leq 2$:

On the other hand, one can explore different *types* of diffusion arising from (1.1). Choosing $p = 2$ results in isotropic diffusion which solves the staircasing problem, but alone is not good for image reconstruction since it has no mechanism for preserving edges. Different values of $1 < p < 2$ result in anisotropic diffusion which is somewhere between TV-based and isotropic smoothing. This type of diffusion can be effective in reconstructing piecewise smooth regions. However, a fixed value of $1 < p < 2$ may not allow for discontinuities, thus obliterating edges. This was shown to be true in the discrete case [15].

Combination of TV-based and isotropic diffusion:

Given the strengths of (1.1) for the different values of p, it seems worthwhile to investigate a model which could self adjust in order to reap the benefits of each. To this end, Chambolle and Lions [4] proposed minimizing the following energy functional which combines isotropic and TV-based diffusion:

$$\min_{u \in H^1(\Omega)} \frac{1}{2\beta} \int_{|\nabla u| \leq \beta} |\nabla u|^2 + \int_{|\nabla u| > \beta} |\nabla u| - \frac{\beta}{2}. \tag{1.2}$$

In this model, the diffusion is strictly perpendicular to the gradient where $|\nabla u| > \beta$; that is, where edges are most likely present, and isotropic where $|\nabla u| \leq \beta$. This model is successful in restoring images where homogeneous regions are separated by distinct edges; however, if the image intensities representing objects are non-uniform or if an image is highly degraded this model may become sensitive to the threshold, β (see figures 5.2, 5.3, and 5.4). In this case, one might want more flexibility when choosing both the direction and speed of diffusion.

Blomgren, Chan, Mulet, and Wong [2] proposed the following minimization problem

$$\min \int_\Omega |\nabla u|^{p(|\nabla u|)} dx$$

where $\lim_{s \to 0} p(s) = 2$, $\lim_{s \to \infty} p(s) = 1$ and p is monotonically decreasing. This model should reap the benefits of both isotropic and TV-based diffusion, as well as a combination of the two. However, it is difficult to study mathematically since the lower semi-continuity of the functional is not readily evident.

1.2. Functionals with $p(x)$ Growth. The model proposed in this paper capitalizes on the strengths of (1.1) for the different values of $1 \leq p \leq 2$. It ensures TV based diffusion ($p \equiv 1$) along edges and Gaussian smoothing ($p \equiv 2$) in homogeneous regions. Furthermore, it employs anisotropic diffusion ($1 < p < 2$) in regions which may be piecewise smooth or in which the difference between noise and edges is difficult to distinguish. We let $p = p(x)$ depend on the location, x, in the image. This way the direction and speed of diffusion at each location depends on the local behavior. Moreover, our choice of exponent yields a model which we can show is theoretically sound.

To this end, the proposed model is as follows:

$$\min_{u \in BV \cap L^2(\Omega)} \int_\Omega \phi(x, Du) + \frac{\lambda}{2}(u - I)^2, \tag{1.3}$$

where

$$\phi(x, r) := \begin{cases} \frac{1}{q(x)} |r|^{q(x)}, & |r| \leq \beta \\ |r| - \frac{\beta q(x) - \beta^{q(x)}}{q(x)}, & |r| > \beta \end{cases} \tag{1.4}$$

where $\beta > 0$ is fixed and $1 < \alpha \leq q(x) \leq 2$. For instance, one can choose

$$q(x) = 1 + \frac{1}{1 + k|\nabla G_\sigma * I(x)|^2} \tag{1.5}$$

where $G_\sigma(x) = \frac{1}{\sigma} exp\left(-|x|^2/4\sigma^2\right)$ is the Gaussian filter and $k > 0$ and $\sigma > 0$ are fixed parameters.

The main benefit of (1.3)-(1.4) is the manner in which it accommodates the local image information. Where the gradient is sufficiently large (i.e. likely edges), only TV-based diffusion will be used. Where the gradient is close to zero (i.e. homogeneous regions), the model is isotropic. At all other locations, the filtering is somewhere between Gaussian and TV-based. Specifically, the type of anisotropy at these ambiguous regions varies according to the strength of the gradient. This enables the model to have a much lower dependence on the threshold (see figures 5.2, 5.3, 5.4, and 5.5).

For several reasons, we've chosen here to prove the well-posedness of the Dirichlet boundary value problem

$$\min_{u\in BV_g\cap L^2(\Omega)} \int_\Omega \phi(x,Du) + \frac{\lambda}{2}(u-I)^2 \tag{1.6}$$

where

$$BV_g(\Omega) := \{u \in BV(\Omega) | u = g \text{ on } \partial\Omega\}, \tag{1.7}$$

and it's associated flow

$$\dot{u} - \operatorname{div}\left(\phi_{\mathrm{r}}(\mathrm{x},\mathrm{Du})\right) + \lambda(\mathrm{u}-\mathrm{I}) = 0, \quad \text{in } \Omega^T \tag{1.8}$$

$$u(x,t) = g(x), \qquad \text{on } \partial\Omega^T \tag{1.9}$$

$$u(0) = I, \qquad \text{in } \Omega \tag{1.10}$$

where

$$\Omega^T := \Omega \times [0,T] \quad \text{and} \quad \partial\Omega^T := \partial\Omega \times [0,T] \tag{1.11}$$

First, the theory is more interesting and challenging mathematically than (1.3). Second, all of the techniques used to study (1.6) also directly solve (1.3). Finally, the Dirichlet problem (1.6) also has direct application in image processing, as it can be used for image interpolation [3, 14], also referred to as noise-free image inpainting [5, 6].

For a special case of (4), where $q(x) \equiv 2$, i.e. $\phi(r) := |r| - \frac{1}{2}$ when $|r| > 1$ and $\phi(r) := \frac{1}{2}|r|^2$ when $|r| \le 1$, the existence, uniqueness and long-time behavior of solutions of (1.6) and it's related flow were studied by Zhou [22]. Later, these results were extended to general convex linear-growth functionals, $\phi = \phi(Du)$ by Hardt and Zhou [11]. In this paper we study the more general case where the functional has non-standard growth. We use a different approximate functional than [22], so different estimates are required. Our analysis is also based on techniques introduced in [7], however, our energy functional requires alternate techniques to establish lower semi-continuity and to pass to the limit from the approximate solution.

The paper is organized as follows. In section 2 we establish some important properties of $\phi(x,Du)$. In section 3 we prove the existence and uniqueness of the solution of the minimization problem (1.6). In section 4 we study the associated evolution problem (1.8)-(1.10). Specifically, we define the notion of a weak solution of (1.8)-(1.10), derive estimates for the solution of an approximating problem, prove existence and uniqueness of the solution of (1.8)-(1.10) and discuss the behavior of the solution as $t \to \infty$. In section 5 we provide our numerical algorithm and experimental results to illustrate the effectiveness of our model in image restoration.

2. Properties of ϕ:. Recall that for $u \in BV(\Omega)$,

$$Du = \nabla u \cdot \mathcal{L}^n + D^s u$$

is a Radon measure, where ∇u is the density of the absolutely continuous part of Du with respect to the n-dimensional Lebesgue measure, $\mathcal{L}^n$, and $D^s u$ is the singular part (see [9]).

Definition 2.1. *For $v \in BV(\Omega)$, define*

$$\int_\Omega \phi(x,Dv) := \int_\Omega \phi(x,\nabla v)dx + \int_\Omega |D^s v|$$

where ϕ is defined as in (1.4). Furthermore, denote

$$\Phi_\lambda(v) := \int_\Omega \phi(x, Dv) + \frac{\lambda}{2}\int_\Omega |v - I|^2 dx, \tag{2.1}$$

$$\Phi_g(v) := \int_\Omega \phi(x, Dv) + \int_{\partial\Omega} |v - g| d\mathcal{H}^{n-1} \tag{2.2}$$

and

$$\Phi_{\lambda,g}(v) := \int_\Omega \phi(x, Dv) + \frac{\lambda}{2}\int_\Omega |v - I|^2 dx + \int_{\partial\Omega} |v - g| d\mathcal{H}^{n-1} \tag{2.3}$$

REMARK 2.2. *For simplicity, we assume that the threshold $\beta = 1$ in (1.4) for all of our theoretical results.*

LEMMA 2.3. *Using the notation in definition 2.1,*

$$\Phi_g(u) = \widetilde{\Phi}_g(u) \tag{2.4}$$

for all $u \in BV(\Omega)$ where

$$\widetilde{\Phi}_g(u) := \sup_{\substack{\psi \in C^1(\overline{\Omega}, \mathbb{R}^n) \\ |\psi| \le 1}} \int_\Omega -u\mathrm{div}\psi - \frac{\mathrm{q(x)} - 1}{\mathrm{q(x)}} |\psi|^{\frac{\mathrm{q(x)}}{\mathrm{q(x)}-1}} \mathrm{dx} + \int_{\partial\Omega} \psi \cdot \mathrm{ngd}\mathcal{H}^{\mathrm{n}-1}.$$

Furthermore, $\Phi_g(u)$ is lower semi-continuous on $L^1(\Omega)$; that is, if $u_j, u \in BV(\Omega)$ satisfy $u_j \to u$ in $L^1(\Omega)$ as $j \to \infty$ then

$$\Phi_g(u) \le \liminf_{j\to\infty} \Phi_g(u_j). \tag{2.5}$$

Proof. First note that for each $\psi \in C^1(\overline{\Omega}, \mathbb{R}^n)$, the map

$$u \longrightarrow \int_\Omega -u\mathrm{div}\psi - \frac{q(x) - 1}{q(x)} |\psi|^{\frac{q(x)}{q(x)-1}} dx + \int_{\partial\Omega} \psi \cdot n g d\mathcal{H}^{n-1}$$

is continuous and affine on $L^1(\Omega)$. Therefore, $\widetilde{\Phi}_g(u)$ is convex and lower semi-continuous on $L^1(\Omega)$ and the domain of $\widetilde{\Phi}_g(u)$, $\{u \,|\, \widetilde{\Phi}_g(u) < \infty\}$, is precisely $BV(\Omega)$.

Now we show that $\Phi_g(u) = \widetilde{\Phi}_g(u)$. For $u \in BV(\Omega)$, we have that for each $\psi \in C^1(\overline{\Omega}, \mathbb{R}^n)$,

$$-\int_\Omega u\mathrm{div}\psi dx = \int_\Omega \nabla u \cdot \psi dx + \int_\Omega D^s u \cdot \psi - \int_{\partial\Omega} u\psi \cdot n d\mathcal{H}^{n-1}$$

and so

$$\widetilde{\Phi}_g(u) = \sup_{\substack{\psi \in C^1(\overline{\Omega}, \mathbb{R}^n) \\ |\psi| \le 1}} \int_\Omega \nabla u \cdot \psi - \frac{q(x) - 1}{q(x)} |\psi|^{\frac{q(x)}{q(x)-1}} dx + \int_\Omega D^s u \cdot \psi - \int_{\partial\Omega} (u - g)\psi \cdot n d\mathcal{H}^{n-1}$$

Since the measures dx, $D^s u$, and $d\mathcal{H}^{n-1}$ are mutually singular, standard arguments show that

$$\widetilde{\Phi}_g(u) = \sup_{\substack{\psi \in C^1(\overline{\Omega}, \mathbb{R}^n) \\ |\psi| \le 1}} \int_\Omega \nabla u \cdot \psi - \frac{q(x) - 1}{q(x)} |\psi|^{\frac{q(x)}{q(x)-1}} dx + \int_\Omega |D^s u| + \int_{\partial\Omega} |u - g| d\mathcal{H}^{n-1}.$$

It only remains to show that

$$\int \phi(x,\nabla u)dx = \sup_{\substack{\psi\in C^1(\overline{\Omega},\mathbb{R}^n)\\ |\psi|\leq 1}} \int \nabla u\cdot\psi - \frac{q(x)-1}{q(x)}|\psi|^{\frac{q(x)}{q(x)-1}}dx. \tag{2.6}$$

Since any $\rho\in L^\infty(\Omega,\mathbb{R}^n)$ can be approximated in measure by $\psi\in C^1(\overline{\Omega},\mathbb{R}^n)$, we have that

$$\sup_{\substack{\psi\in C^1(\overline{\Omega},\mathbb{R}^n)\\ |\psi|\leq 1}} \int_\Omega \nabla u\cdot\psi - \frac{q(x)-1}{q(x)}|\psi|^{\frac{q(x)}{q(x)-1}}dx = \sup_{\substack{\rho\in L^\infty(\Omega,\mathbb{R}^n)\\ |\rho|\leq 1}} \int_\Omega \nabla u\cdot\rho - \frac{q(x)-1}{q(x)}|\rho|^{\frac{q(x)}{q(x)-1}}dx. \tag{2.7}$$

Choosing $\rho(x) = 1_{\{|\nabla u|\leq 1\}}|\nabla u|^{q(x)-1}\frac{\nabla u}{|\nabla u|} + 1_{\{|\nabla u|>1\}}\frac{\nabla u}{|\nabla u|}$, where 1_E is the indicator function on E, we see that the right hand side of (2.7) is

$$\geq \int_\Omega \frac{1}{q(x)}|\nabla u|^{q(x)}1_{\{|\nabla u|\leq 1\}} + \left[|\nabla u| - \frac{q(x)-1}{q(x)}\right]1_{\{|\nabla u|>1\}}dx = \int_\Omega \phi(x,\nabla u)dx. \tag{2.8}$$

To show equality, we proceed as follows. For any $\rho\in L^\infty(\Omega,\mathbb{R}^n)$, since $q(x)>1$ we have that for almost all x,

$$\nabla u(x)\cdot\rho(x) \leq \frac{1}{q(x)}|\nabla u|^{q(x)} + \frac{q(x)-1}{q(x)}|\rho(x)|^{\frac{q(x)}{q(x)-1}}$$

In particular, if $|\nabla u|\leq 1$,

$$\nabla u(x)\cdot\rho(x) - \frac{q(x)-1}{q(x)}|\rho(x)|^{\frac{q(x)}{q(x-1)}} \leq \frac{1}{q(x)}|\nabla u|^{q(x)} \tag{2.9}$$

Finally, we claim that if $|\nabla u|>1$,

$$\nabla u(x)\cdot\rho(x) - \frac{q(x)-1}{q(x)}|\rho(x)|^{\frac{q(x)}{q(x)-1}} \leq |\nabla u| - \frac{q(x)-1}{q(x)} \tag{2.10}$$

Indeed, if $|\nabla u|>1$ and $|\rho|\leq 1$,then since $q(x)>1$ for almost all x we have that

$$\nabla u\cdot\rho = |\nabla u|\frac{\nabla u}{|\nabla u|}\cdot\rho \leq |\nabla u|\left[\frac{1}{q(x)} + \frac{q(x)-1}{q(x)}|\rho|^{\frac{q(x)}{q(x)-1}}\right]$$

and so

$$\nabla u\cdot\rho - \frac{q(x)-1}{q(x)}|\rho|^{\frac{q(x)}{q(x)-1}} \leq \frac{1}{q(x)}|\nabla u| + (|\nabla u|-1)\frac{q(x)-1}{q(x)}|\rho|^{\frac{q(x)}{q(x)-1}} \leq |\nabla u| - \frac{q(x)-1}{q(x)}$$

Combining, (2.7), (2.8), (2.9), and (2.10), we have that

$$\sup_{\substack{\psi\in C^1(\overline{\Omega},\mathbb{R}^n)\\ |\psi|\leq 1}} \int_\Omega \nabla u\cdot\psi - \frac{q(x)-1}{q(x)}|\psi|^{\frac{q(x)}{q(x)-1}}dx = \int_\Omega \phi(x,\nabla u)dx$$

and so for all $u\in BV(\Omega)$, $\widetilde{\Phi}_g(u) = \Phi_g(u)$ where Φ_g is defined in (2.2). □

LEMMA 2.4. *Suppose $\Omega\subset\mathbb{R}^n$ is open, bounded and has Lipschitz boundary and let $w\in BV\cap L^2(\Omega)$. Then for each $\delta>0$ there exists $\tilde{w}_\delta\in C^\infty\cap H^1(\Omega)$ such that*

$$\Phi_{\lambda,g}(\tilde{w}_\delta) \leq \Phi_{\lambda,g}(w) + \delta. \tag{2.11}$$

Furthermore, if we also assume that $Trw = TrG$ in $L^1(\partial\Omega)$ for some $G \in H^1(\Omega)$, then for each $\delta > 0$, there exists $w_\delta \in H^1(\Omega)$ satisfying

$$Trw_\delta = Trw \text{ in } L^1(\partial\Omega), \tag{2.12}$$

$$w_\delta \to w \text{ strongly in } L^2(\Omega) \text{ as } \delta \to 0, \text{ and} \tag{2.13}$$

$$\Phi_{\lambda,g}(w_\delta) \leq \Phi_{\lambda,g}(w) + \delta. \tag{2.14}$$

where TrG is the trace of G on $\partial\Omega$.

Proof. : Fix $w \in BV \cap L^2(\Omega)$. Using lemma 2.3 and a slight modification of the proof of Theorem 1.17 and Remark 1.18 in [10], there exists a sequence $\{w_j\}$ in $C^\infty \cap H^1(\Omega)$ such that

$$Trw_j = Trw \text{ in } L^1(\partial\Omega) \text{ and} \tag{2.15}$$

$$w_j \to w \text{ in } L^2(\Omega) \text{ and} \tag{2.16}$$

$$\lim_{j\to\infty} \Phi_g(w_j) = \Phi_g(w). \tag{2.17}$$

Therefore, for each $\delta > 0$ there exists a function $\tilde{w}_\delta \in C^\infty \cap H^1(\Omega)$ such that

$$\Phi_{\lambda,g}(\tilde{w}_\delta) \leq \Phi_{\lambda,g}(w) + \delta \tag{2.18}$$

and (2.11) holds.

Now suppose also that $Trw = TrG$ in $L^1(\partial\Omega)$. Then by (2.15), $\tilde{w}_\delta - G \in H_0^1(\Omega)$, so there exists a function $h_\delta \in C_0^\infty(\Omega)$ such that

$$||\tilde{w}_\delta - G - h_\delta||_{H^1(\Omega)} + ||\tilde{w}_\delta - G - h_\delta||_{L^2(\Omega)} \leq \delta \tag{2.19}$$

Let $w_\delta = G + h_\delta \in H^1(\Omega)$. Then we have that

$$\begin{gathered} Trw_\delta = Trw \text{ in } L^1(\partial\Omega), \\ w_\delta \to w \text{ in } L^2(\Omega) \text{ as } \delta \to 0, \text{ and} \\ \Phi_{\lambda,g}(w_\delta) \leq \Phi_{\lambda,g}(w) + \delta. \end{gathered}$$

and the proof is complete. □

Remark 2.5. *If $w \in BV \cap L^\infty(\Omega)$, then there exist $w_\delta \in H^1 \cap L^\infty(\Omega)$ such that in addition to (2.12)-(2.14), we also have that*

$$||w_\delta||_{L^\infty(\Omega)} \leq C(\Omega)||w||_{L^\infty(\Omega)} \tag{2.20}$$

3. The Minimization Problem. In this section we study the existence and uniqueness of the solution to the minimization problem (1.6). In general, as discussed in [11], [13] and [22], there may not exist a minimizer of $\Phi_\lambda(v)$, defined in (2.1), since the limit of the minimizing sequence may not take the boundary value g. However, we can prove the existence of a unique minimizer for a weaker form of (1.6) where we consider the minimization problem using the *relaxed energy*, $\Phi_{\lambda,g}(v)$, defined in (2.3). Specifically, we define a pseudosolution of (1.6) as follows.

Definition 3.1. *A function $u \in BV \cap L^2(\Omega)$ is a pseudosolution of* (1.6) *if it is a solution of*

$$\min_{v\in BV\cap L^2(\Omega)} \Phi_{\lambda,g}(v) \tag{3.1}$$

where $\Phi_{\lambda,g}(v)$ is defined in equation (2.3).

First we show that there exists a pseudosolution of (1.6), that is, a solution of (3.1), in Theorem 3.2. Then, in Theorem 3.5 we provide the motivation for using the notion of pseudosolution in definition 3.1.

THEOREM 3.2. *Suppose $I \in BV \cap L^2(\Omega)$, $g = TrG$ for some function $G \in H^1(\Omega)$ with $I = g$ on $\partial\Omega$, and Ω is an open bounded subset of $\mathbb{R}^n$ with Lipschitz boundary. Then there exists a unique pseudosolution of* (1.6) *as given in definition 3.1.*

Proof. : Let $\{u_n\}$ be a minimizing sequence of (3.1) in $BV \cap L^2(\Omega)$. Since $\{u_n\}$ is bounded in $BV(\Omega)$ and $L^2(\Omega)$, using the compactness of $BV(\Omega)$ and the weak compactness of $L^2(\Omega)$, there exists a subsequence $\{u_{n_k}\}$ of $\{u_n\}$ and a function $u \in BV \cap L^2(\Omega)$ satisfying

$$u_{n_k} \to u \text{ strongly in } L^1(\Omega) \tag{3.2}$$
$$u_{n_k} \rightharpoonup u \text{ weakly in } L^2(\Omega). \tag{3.3}$$

By (3.2), (3.3), lemma 2.3 and the weak lower semi-continuity of the L^2-norm, we have that

$$\Phi_{\lambda,g}(u) \leq \liminf_{k\to\infty} \Phi_{\lambda,g}(u_{n_k}) = \inf_{BV\cap L^2(\Omega)} \Phi_{\lambda,g}(v).$$

Hence, u is a solution of the minimization problem. Uniqueness follows from the strict convexity of $\Phi_{\lambda,g}(v)$ in v. □

To show (3.7) holds, we need the following two lemmas. For $\beta > 0$, let

$$d_\beta(x) = \min\left(\frac{d(x)}{\beta}, 1\right), \tag{3.4}$$

where $d(x)$ is the distance of the point x to the boundary of Ω.

LEMMA 3.3. *(Theorem A.1 [7]): For each $v \in BV \cap L^\infty(\Omega)$, the vector measures $v\nabla d_\beta$ converge weakly to $-v\gamma d\mathcal{H}^{n-1}$ as $\beta \to 0$, where γ is the unit outward normal to $\partial\Omega$, and*

$$\lim_{\beta\to 0} \int_\Omega |v||\nabla d_\beta| = \int_{\partial\Omega} |v| d\mathcal{H}^{n-1}.$$

LEMMA 3.4. *Let $G \in H^1 \cap L^\infty(\Omega)$. Then for any $v \in BV \cap L^\infty(\Omega)$, there exists a sequence $\{v_\beta\}$ in $BV \cap L^\infty(\Omega)$ such that*

$$Trv_\beta = TrG \text{ in } L^1(\partial\Omega),$$
$$v_\beta \to v \text{ in } L^2(\Omega) \text{ as } \beta \to 0, \text{ and}$$
$$\lim_{\beta\to 0} \Phi_g(v_\beta) = \Phi_g(v).$$

Proof. : For $\beta > 0$, define $d_\beta(x)$ as in (3.4). Since $d(x) \in W^{1,\infty}(\Omega)$ and $|\nabla d| = 1$, we have that

$$|\nabla d_\beta| = \frac{1}{\beta} \text{ if } d(x) < \beta \text{ and } |\nabla d_\beta| = 0 \text{ if } d(x) \geq \beta \tag{3.5}$$

Fix $v \in BV \cap L^\infty(\Omega)$ and let $v_\beta = d_\beta v + (1 - d_\beta)G$ for $(x,t) \in \Omega$. Then

$$v_\beta \in BV \cap L^\infty(\Omega) \text{ with } Trv_\beta = TrG \text{ in } L^1(\partial\Omega),$$
$$v_\beta \to v \text{ in } L^2(\Omega)$$

By lemma 2.3, $\liminf_{\beta\to 0} \Phi_g(v_\beta) \geq \Phi_g(v)$, so it only remains to show that

$$\lim_{\beta\to 0} \Phi_g(v_\beta) \leq \Phi_g(v). \tag{3.6}$$

Writing $\Phi_g = \widetilde{\Phi}_g$ (lemma 2.3), since $D^s v_\beta = d_\beta D^s v$ and $Tr v_\beta = TrG$ in $L^1(\partial\Omega)$ we have that

$$\widetilde{\Phi}_g(v_\beta) = \sup_{\substack{\psi\in C^1(\overline{\Omega},\mathbb{R}^n)\\ |\psi|\le 1}} \left[\int_\Omega \{(v-G)\nabla d_\beta + d_\beta \nabla v + (1-d_\beta)\nabla G\}\cdot\psi - \frac{q(x)-1}{q(x)}|\psi|^{\frac{q(x)}{q(x)-1}}dx + \int_\Omega d_\beta D^s v\cdot\psi\right]$$

Therefore, by (2.6)

$$\begin{aligned}\widetilde{\Phi}(v_\beta) &\le \sup_{\substack{\psi\in C^1(\overline{\Omega},\mathbb{R}^n)\\ |\psi|\le 1}} \left[\int_\Omega \nabla v\cdot\psi - \frac{q(x)-1}{q(x)}|\psi|^{\frac{q(x)}{q(x)-1}}dx\right]\\ &\quad + \int_\Omega |v-G||\nabla d_\beta|dx + \int_\Omega (1-d_\beta)(|\nabla v| + |\nabla G|)dx + \int_\Omega d_\beta |D^s v|\\ &= \int_\Omega \phi(x,\nabla v) + \int_\Omega |v-G||\nabla d_\beta|dx + \int_\Omega (1-d_\beta)(|\nabla v| + |\nabla G|)dx + \int_\Omega d_\beta|D^s v|\end{aligned}$$

By lemma 3.3, as $\beta\to 0$,

$$\int_\Omega |v-G||\nabla d_\beta|dx \to \int_{\partial\Omega}|v-G|d\mathcal{H}^{n-1}.$$

Furthermore, the Lebesgue Dominated Convergence Theorem gives us that

$$\begin{aligned}&\int_\Omega (1-d_\beta)(|\nabla v| + |\nabla G|)dx \to 0\\ &\text{and } \int_\Omega d_\beta |D^s v| \to \int_\Omega |D^s v|.\end{aligned}$$

Therefore, (3.6) holds and the lemma is proved. □

THEOREM 3.5.

$$\inf_{v\in BV_g\cap L^2(\Omega)} \Phi_\lambda(v) = \inf_{v\in BV\cap L^2(\Omega)} \Phi_{\lambda,g}(v), \tag{3.7}$$

where Φ_λ and $\Phi_{\lambda,g}$ are defined in (2.1) *and* (2.3) *respectively and BV_g is defined in* (1.7).

Proof. : Since $BV_g(\Omega)\subset BV(\Omega)$

$$\inf_{v\in BV\cap L^2(\Omega)} \Phi_{\lambda,g}(v) \le \inf_{v\in BV_g\cap L^2(\Omega)} \Phi_{\lambda,g}(v) = \inf_{v\in BV_g\cap L^2(\Omega)} \Phi_\lambda(v).$$

To see the reverse, let $u\in BV\cap L^2(\Omega)$ be the solution of (3.1); that is,

$$\Phi_{\lambda,g}(u) = \min_{v\in BV\cap L^2(\Omega)} \Phi_{\lambda,g}(v).$$

By lemma 3.4, there exist $v_\beta \in BV_g\cap L^\infty(\Omega)$ such that

$$\Phi_\lambda(v_\beta) = \Phi_{\lambda,g}(v_\beta) \overset{\beta\to 0}{\longrightarrow} \Phi_{\lambda,g}(u) = \min_{v\in BV\cap L^2(\Omega)} \Phi_{\lambda,g}(v)$$

and so

$$\inf_{v\in BV_g\cap L^2(\Omega)} \Phi_\lambda(v) \le \min_{v\in BV\cap L^2(\Omega)} \Phi_{\lambda,g}(v).$$

Thus, the theorem holds. □

4. The Flow related to the Minimization Problem (3.1).

4.1. Motivation for the Weak Solution.
Suppose that

$$v \in L^2(0,T;H^1(\Omega)) \tag{4.1}$$

and that u is a classical solution of (1.8)-(1.10). Multiplying (1.8) by $(v-u)$, integrating over Ω, and using the convexity of ϕ we have that

$$\int_\Omega \dot{u}(v-u)dx + \Phi_{\lambda,g}(v) \geq \Phi_{\lambda,g}(u) \tag{4.2}$$

Integrating over $[0,s]$ for any $s \in [0,T]$ then yields

$$\int_0^s \int_\Omega \dot{u}(v-u)dxdt + \int_0^s \Phi_{\lambda,g}(v)dt \geq \int_0^s \Phi_{\lambda,g}(u)dt \tag{4.3}$$

On the other hand, setting $v = u + \epsilon w$ in (4.3) with $w \in C_0^\infty(\Omega)$ makes it clear that

$$\int_0^s \int_\Omega \dot{u}(\epsilon w)dxdt + \int_0^s \Phi_{\lambda,g}(u+\epsilon w)dt$$

attains a minimum at $\epsilon = 0$. Therefore, if u satisfies (4.3) and $u \in L^2(0,T;BV \cap L^2(\Omega))$ with $\dot{u} \in L^2(\Omega^T)$, u is also a solution of (1.8)-(1.10) in the sense of distribution. This motivates the following definition:

Definition 4.1. *We say that a function $u \in L^2(0,T;BV \cap L^2(\Omega))$ with $\dot{u} \in L^2(\Omega^T)$ is a pseudosolution of (1.8)-(1.10) if*

1. *$u(x,0) = I(x)$ on Ω, and*
2. *u satisfies (4.3) for all $s \in [0,T]$ and $v \in L^2(0,T;BV \cap L^2(\Omega))$.*

4.2. The Approximate Functional, ϕ^ϵ.

For $\epsilon > 0$, define

$$\phi^\epsilon(x,r) := \begin{cases} \frac{1}{q(x)}|r|^{q(x)}, & |r| \leq 1 \\ \frac{1}{1+\epsilon}|r|^{(1+\epsilon)} - \frac{q(x)-(1+\epsilon)}{(1+\epsilon)q(x)}, & |r| > 1 \end{cases} \tag{4.4}$$

Remark 4.2. *We note the following properties, as they will be useful in later computations.*

1. *$\phi^\epsilon(x,r)$ is convex in r.*
2. *$\phi^\epsilon_r(x,r) \cdot r \geq 0$ for all $r \in \mathbb{R}^n$;*
3. *$\phi(x,r) \leq \phi^\epsilon(x,r)$ for all $r \in \mathbb{R}^n$.*

To prove the existence and uniqueness of the pseudosolution of (1.8)-(1.10), we first study solutions of the approximate problem

$$\dot{u} - \epsilon\Delta u - \operatorname{div}(\phi^\epsilon_{\mathrm{r}}(\mathrm{x},\nabla \mathrm{u})) + \lambda(\mathrm{u}-\mathrm{I}) = 0, \quad \text{in } \Omega \times [0,T] \tag{4.5}$$

$$u(x,t) = g(x), \qquad \text{in } \partial\Omega \times [0,T] \tag{4.6}$$

$$u(x,0) = \tilde{I}(x), \qquad \text{in } \Omega \tag{4.7}$$

where $\tilde{I} \in H^1 \cap L^\infty(\Omega)$, $g \in L^\infty(\partial\Omega)$ with $g = TrG$ in $L^1(\partial\Omega)$ for some $G \in H^1(\Omega)$, and $\tilde{I}|_{\partial\Omega} = g$.

Lemma 4.3. *Suppose $\tilde{I} \in H^1(\Omega)$ with $\tilde{I}|_{\partial\Omega} = g$. Then the problem (4.5)-(4.7) has a unique solution $u \in L^2(0,T;H^1(\Omega)) \cap C(0,T;L^2(\Omega))$ with $\dot{u} \in L^2(0,T;L^2(\Omega))$ such that*

$$\int_0^\infty \int_\Omega |\dot{u}|^2 dxdt + \sup_{t>0}\left[\int_\Omega \frac{\epsilon}{2}|\nabla u|^2 + \phi^\epsilon(x,\nabla u) + \frac{\lambda}{2}|u-\tilde{I}|^2\right] \leq \frac{\epsilon}{2}\int_\Omega |\nabla\tilde{I}|^2 + \phi^\epsilon(x,\nabla\tilde{I})dx \tag{4.8}$$

Proof. : Since (4.5) is uniformly parabolic, we can conclude this lemma by standard results for parabolic equations [12] and the corresponding energy estimate. □

4.3. Estimates for the Solution of the Approximate Problem.

LEMMA 4.4. *If $\tilde{I} \in H^1 \cap L^\infty \cap BV(\Omega)$, $g \in L^\infty(\partial\Omega)$ with $\tilde{I}|_{\partial\Omega} = g$, and u is a solution of (4.5)-(4.7), then*

$$||u||_{L^\infty(\Omega^T)} \leq \max(||\tilde{I}||_{L^\infty(\Omega)}, ||g||_{L^\infty(\partial\Omega)}) \tag{4.9}$$

Proof. : Let $M := \max(||\widetilde{I}||_{L^\infty(\Omega)}, ||g||_{L^\infty(\partial\Omega)})$. Multiply (4.5) by $(u-M)_+$, where

$$(u-M)_+ = \begin{cases} u-M & \text{if } u-M \geq 0 \\ 0 & \text{otherwise} \end{cases}$$

and integrate over Ω to get

$$\int_\Omega \dot{u}(u-M)_+ dx + \epsilon \int_\Omega |\nabla u|^2 dx + \int_\Omega \phi_r^\epsilon(x, \nabla u) \cdot \nabla u dx + \lambda \int_\Omega (u - \tilde{I})(u-M)_+ dx = 0 \tag{4.10}$$

By Remark 4.2 (2) we have that $\int_\Omega \phi_r^\epsilon(x, \nabla u) \cdot \nabla u dx \geq 0$ and so

$$\frac{1}{2} \int_\Omega \frac{d}{dt}(u-M)_+^2 dx \leq 0$$

Therefore, $\frac{1}{2}\int_\Omega (u-M)_+^2 dx$ is decreasing in t and since

$$\frac{1}{2}\int_\Omega (u-M)_+^2 dx \geq 0 \text{ and } \frac{1}{2}\int_\Omega (\mathrm{u}-\mathrm{M})_+^2 \mathrm{dx}|_{\mathrm{t}=0} = 0,$$

we have that

$$\frac{1}{2}\int_\Omega (u-M)_+^2 dx = 0 \text{ for all t} \in [0, \mathrm{T}]$$

and so

$$u(t) \leq M = \max(||\tilde{I}||_{L^\infty(\Omega)}, ||g||_{L^\infty(\partial\Omega)}) \ \mathcal{L} - a.e. \text{ on } \Omega \ \forall \mathrm{t} > 0.$$

Multiplying (4.5) by $(u+M)_+$, a similar argument yields that $u(t) \geq -M$ for all t. (4.9) follows directly. □

LEMMA 4.5. *Let u be the solution of (4.5)-(4.7). Then for all $v \in L^2(0,T; H^1(\Omega))$ with $v|_{\partial\Omega} = g$,*

$$\begin{aligned} &\int_0^s \int_\Omega \dot{u}(v-u) + \frac{\epsilon}{2}|\nabla v|^2 + \phi^\epsilon(x, Dv) + \frac{\lambda}{2}|v - \tilde{I}|^2 dx dt \\ &\quad \geq \int_0^s \int_\Omega \frac{\epsilon}{2}|\nabla u|^2 + \phi^\epsilon(x, Du) + \frac{\lambda}{2}|u - \tilde{I}|^2 dx dt \end{aligned} \tag{4.11}$$

Proof. : Multiplying (4.5) by $v-u$, then integrating by parts and using the convexity of $\phi^\epsilon(x,r)$ in r, (4.11) follows. □

REMARK 4.6. *Let u be the solution of (4.5)-(4.7). Then for any $0 < \epsilon < \alpha - 1$ (where $1 < \alpha \leq q(x)$) we have the following estimate which is a direct consequence of lemma 4.3:*

$$\int_0^\infty \int_\Omega |\dot{u}|^2 dx dt + \sup_{t>0}\left[\int_\Omega \frac{1}{1+\epsilon}|\nabla u|^{1+\epsilon} dx + \frac{\lambda}{2}\int_\Omega |u - \tilde{I}|^2 dx\right] \leq C \tag{4.12}$$

where $C > 0$ is a constant depending only on Ω and $||\nabla \tilde{I}||_{L^2(\Omega)}$.

4.4. Existence and Uniqueness of (1.8)-(1.10).

Since $I \in BV \cap L^\infty(\Omega)$, by lemma 2.4 and remark 2.5 there exists a sequence $\{I_\delta\}$ in $H^1 \cap L^\infty(\Omega)$ such that

$$TrI_\delta = TrI \text{ on } \partial\Omega, \tag{4.13}$$

$$||I_\delta||_{L^\infty(\Omega)} \leq C||I||_{L^\infty(\Omega)}, \tag{4.14}$$

$$I_\delta \to I \text{ strongly in } L^2(\Omega) \text{ as } \delta \to 0, \text{ and} \tag{4.15}$$

$$\Phi_{\lambda,g}(I_\delta) \leq \Phi_{\lambda,g}(I) + \delta. \tag{4.16}$$

THEOREM 4.7. *(**Existence and Uniqueness**) Suppose $I \in BV \cap L^\infty(\Omega)$, $g \in L^\infty(\partial\Omega)$ and $I|_{\partial\Omega} = g$ with $g = TrG$ for some function $G \in H^1(\Omega)$. Then there exists a unique pseudosolution $u \in L^\infty(0,\infty; BV \cap L^\infty(\Omega))$ of (1.8)-(1.10).*

Proof. : 1. First we fix $\delta > 0$ and pass to the limit $\epsilon \to 0$.

Let $\{u_\delta^\epsilon\}$ be the sequence of solutions to (4.5)-(4.7) with initial data $\tilde{I} = I_\delta$. By lemma 4.4 and remark 4.6, there exists a subsequence $\{u_\delta^{\epsilon_i}\}$ and a function $u_\delta \in L^\infty(\Omega^\infty)$ with $\dot{u}_\delta \in L^2(\Omega^\infty)$ such that as $\epsilon_i \to 0$,

$$u_\delta^{\epsilon_i} \rightharpoonup u_\delta \text{ weakly}^* \text{ in } L^\infty(\Omega^\infty) \tag{4.17}$$

$$\dot{u}_\delta^{\epsilon_i} \rightharpoonup w \text{ weakly in } L^2(\Omega^\infty) \tag{4.18}$$

The same argument used in the proof of lemma 3.1 in [22] gives us that $\dot{u}_\delta = w$ and $u_\delta(0) = I_\delta$.

Moreover, for all $f \in L^2(\Omega)$,

$$\int_\Omega (u_\delta^{\epsilon_i}(\cdot,t) - I_\delta) f(x)dx = \int_0^t \int_\Omega \dot{u}_\delta^{\epsilon_i}(x,s) 1_{[0,t]}(s) f(x)dxds$$

$$\xrightarrow{\epsilon_i \to 0} \int_0^t \int_\Omega \dot{u}_\delta(x,s) 1_{[0,t]}(s) f(x)dxds = \int_\Omega (u_\delta(\cdot,t) - I_\delta) f(x)dx.$$

Therefore, for each $t > 0$,

$$u_\delta^{\epsilon_i}(\cdot,t) \rightharpoonup u_\delta(\cdot,t) \text{ weakly in } L^2(\Omega) \tag{4.19}$$

From (4.12), for each $t > 0$, $\{u_\delta^{\epsilon_i}\}$ is a bounded sequence in $W^{1,1}(\Omega)$. Therefore, there exists a convergent subsequence $\{u_\delta^{\epsilon_{i_j}}\}$ of $\{u_\delta^{\epsilon_i}\}$ such that

$$u_\delta^{\epsilon_{i_j}}(\cdot,t) \to u_\delta(\cdot,t) \text{ strongly in } L^1(\Omega)$$

Note that every convergent subsequence of $\{u_\delta^{\epsilon_i}\}$ converges to the same limit $u_\delta(\cdot,t)$ due to (4.19). Then, for each $t > 0$,

$$u_\delta^{\epsilon_i}(\cdot,t) \to u_\delta(\cdot,t) \text{ strongly in } L^1(\Omega) \tag{4.20}$$

From (4.17) and (4.20), we have that for each $t > 0$,

$$u_\delta^{\epsilon_i}(\cdot,t) \to u_\delta(\cdot,t) \text{ strongly in } L^2(\Omega) \tag{4.21}$$

We also have from (4.12) and (4.20) that $u_\delta \in L^\infty(0,\infty, BV \cap L^\infty(\Omega))$ with $\dot{u}_\delta \in L^2(\Omega^\infty)$. Furthermore, by lemma 4.5, for all $v \in L^2(0,T; H^1(\Omega))$ with $v|_{\partial\Omega} = g$,

$$\int_0^s \int_\Omega \dot{u}_\delta^{\epsilon_i}(v - u_\delta^{\epsilon_i}) + \frac{\epsilon_i}{2}|\nabla v|^2 + \phi^{\epsilon_i}(x, \nabla v) + \frac{\lambda}{2}|v - I_\delta|^2 dxdt$$

$$\geq \int_0^s \int_\Omega \frac{\epsilon_i}{2}|\nabla u_\delta^{\epsilon_i}|^2 + \phi^{\epsilon_i}(x, Du_\delta^{\epsilon_i}) + \frac{\lambda}{2}|u_\delta^{\epsilon_i} - I_\delta|^2 dxdt \tag{4.22}$$

Using (4.18) and (4.21), we can let $\epsilon_i \to 0$ in (4.22) to get

$$\int_0^s \int_\Omega \dot{u}_\delta(v-u_\delta) + \phi(x,\nabla v) + \frac{\lambda}{2}|v-I_\delta|^2 dxdt \tag{4.23}$$
$$\geq \lim_{\epsilon_i \to 0} \int_0^s \int_\Omega \phi^{\epsilon_i}(x, Du_\delta^{\epsilon_i})dxdt + \frac{\lambda}{2}\int_0^s \int_\Omega |u_\delta - I_\delta|^2 dxdt$$

By lemma 2.3, w.l.s.c. and Remark 4.2 (3),

$$\lim_{\epsilon_i \to 0} \int_0^s \int_\Omega \phi^{\epsilon_i}(x, Du_\delta^{\epsilon_i})dxdt \geq \int_0^s \int_\Omega \phi(x, Du_\delta)dxdt + \int_0^s \int_{\partial\Omega} |u_\delta - g| d\mathcal{H}^{n-1}dt \tag{4.24}$$

The combination of (4.23) and (4.24) gives us

$$\int_0^s \int_\Omega \dot{u}_\delta(v-u_\delta) + \phi(x,\nabla v) + \frac{\lambda}{2}|v-I_\delta|^2 dxdt + \int_0^s \int_{\partial\Omega} |v-g| d\mathcal{H}^{n-1}dt$$
$$\geq \int_0^s \int_\Omega \phi(x,\nabla u_\delta) + \frac{\lambda}{2}|u_\delta - I_\delta|^2 dxdt + \int_0^s \int_{\partial\Omega} |u_\delta - g| d\mathcal{H}^{n-1}dt \tag{4.25}$$

for all $v \in L^2(0,\infty; H^1(\Omega))$ with $v = g$ on $\partial\Omega^\infty$. By approximation, (4.25) still holds for $v \in L^2(0,\infty; BV \cap L^\infty(\Omega))$ with $v = g$ on $\partial\Omega^\infty$. To see that (4.25) holds for all $v \in L^2(0,\infty; BV \cap L^\infty(\Omega))$ (in particular, without $v = g$ on $\partial\Omega^\infty$), replace v by $v_\beta = d_\beta v + (1-d_\beta)G$ in (4.25) and (by lemma 3.4) let $\beta \to 0$. By approximation, we can conclude that (4.25) holds for all $v \in L^2(0,\infty; BV \cap L^2(\Omega))$.

2. Now it only remains to pass to the limit as $\delta \to 0$ in (4.25) to complete the proof.

First note that (4.8) holds for $u_\delta^{\epsilon_i}$ with $\tilde{I} = I_\delta$. Fix $\delta > 0$. By w.l.s.c. and (4.20), the same argument used to deduce (4.24) also gives us that

$$\lim_{\epsilon_i \to 0} \int_\Omega \phi^{\epsilon_i}(x, Du_\delta^{\epsilon_i})dx \geq \int_\Omega \phi(x, Du_\delta)dx + \int_{\partial\Omega} |u_\delta - g| d\mathcal{H}^{n-1}.$$

Therefore, we can pass to the limit as $\epsilon_i \to 0$ in (4.8) and get

$$\int_0^\infty \int_\Omega |\dot{u}_\delta|^2 dxdt + \sup_{t>0}\left[\int_\Omega \phi(x, Du_\delta)dxdt + \frac{\lambda}{2}|u_\delta - I_\delta|^2 + \int_{\partial\Omega} |u_\delta - g| d\mathcal{H}^{n-1}dt\right] \leq \int_\Omega \phi(x,\nabla I_\delta)dx \tag{4.26}$$

Then $\{u_\delta\}$ is uniformly bounded in $W^{1,1}(\Omega)$ for each $t > 0$. Note also that in lemma 4.4 the bound is independent of both ϵ and δ. Therefore, $\{u_\delta\}$ is also uniformly bounded in $L^\infty(\Omega^\infty)$. From (4.26), we also have $\{\dot{u}_\delta\}$ is uniformly bounded in $L^2(\Omega^\infty)$.

By the same argument used to obtain (4.17), (4.18), and (4.21), there exists a subsequence $\{u_{\delta_j}\}$ of $\{u_\delta\}$ and a function $u \in L^\infty(0,\infty, BV \cap L^\infty(\Omega))$ with $\dot{u} \in L^2(\Omega^\infty)$ such that as $\delta_j \to 0$,

$$u_{\delta_j} \rightharpoonup u \text{ weakly}^* \text{ in } L^\infty(\Omega^\infty) \tag{4.27}$$
$$\dot{u}_{\delta_j} \rightharpoonup \dot{u} \text{ weakly in } L^2(\Omega^\infty) \tag{4.28}$$
$$u_{\delta_j}(\cdot,t) \to u(\cdot,t) \text{ strongly in } L^2(\Omega) \text{ and uniformly in } t \tag{4.29}$$

Let $\delta = \delta_j$ in (4.25). Using w.l.s.c. and (4.27)-(4.29), we can let $\delta_j \to 0$ in (4.25) to conclude that for all $v \in L^2(0,\infty, BV \cap L^2(\Omega))$,

$$\int_0^s \int_\Omega \dot{u}(v-u)dxdt + \int_0^s \Phi_{\lambda,g}(v)dt \geq \int_0^s \Phi_{\lambda,g}(u)dt.$$

Existence is proved.

4. (Uniqueness) Suppose that u_1, u_2 are both weak solution of (1.8)-(1.10). As in [11] and [22], we can obtain two inequalities: the first by setting $u = u_1$ and $v = u_2$ in (4.3) and the second by setting $u = u_2$ and $v = u_1$. Adding these two inequalities gives us that for all $s > 0$,

$$\int_0^s \int_\Omega \frac{1}{2}\frac{d}{dt}|u_1 - u_2|^2 dxdt \leq 0.$$

Therefore, $u_1 = u_2$ in Ω^∞. □

4.5. Behavior as $t \to \infty$.

THEOREM 4.8. *As $t \to \infty$, the weak solution, $u(x,t)$, of (1.8)-(1.10) converges strongly in $L^2(\Omega)$ to a minimizer $\tilde{u}$ of the function $\Phi_{\lambda,g}$; i.e., the pseudosolution, $\tilde{u}$, of* (3.1)

Proof. : Since u satisfies (4.3), for any $s > 0$ we can substitute $v(x) \in BV \cap L^2(\Omega)$ into (4.3):

$$\int_\Omega (u(x,s) - I(x))v(x)dx - \frac{1}{2}\int_\Omega (u^2(x,s) - I^2(x))dx + s\int_\Omega \phi(x,\nabla v) + s\frac{\lambda}{2}\int_\Omega |v - I|^2 dx + s\int_{\partial\Omega} |v - g| d\mathcal{H}^{n-1}$$
$$\geq \int_0^s \int_\Omega \phi(x,\nabla u)dt + \frac{\lambda}{2}\int_0^s \int_\Omega |u - I|^2 dxdt + \int_0^s \int_{\partial\Omega} |u - g| d\mathcal{H}^{n-1} dt \quad (4.30)$$

Proceeding as in [7], let

$$w(x,s) = \frac{1}{s}\int_0^s u(x,t)dt.$$

Since $u \in L^\infty(0,\infty; BV \cap L^\infty(\Omega))$, for each $s > 0$ we have that $w(\cdot,s) \in BV \cap L^\infty(\Omega)$ with $\{w(\cdot,s)\}$ uniformly bounded in $BV(\Omega)$ and $L^\infty(\Omega)$. Therefore, there exists a subsequence $\{w(\cdot,s_i)\}$ of $\{w(\cdot,s)\}$ which converges strongly in $L^1(\Omega)$ and weakly in $BV(\Omega)$ and $L^\infty(\Omega)$ to a function $\tilde{u} \in BV \cap L^\infty(\Omega)$ as $s_i \to \infty$. Since $\{w(\cdot,s)\}$ is uniformly bounded in $L^\infty(\Omega)$, $\{w(\cdot,s_i)\}$ also converges strongly in $L^2(\Omega)$ to $\tilde{u}$.

Dividing (4.5) by s and taking the limit along $s_i \to \infty$ gives us that

$$\int_\Omega \phi(x,\nabla v) + \frac{\lambda}{2}\int_\Omega |v - I|^2 dx + \int_{\partial\Omega} |v - g| d\mathcal{H}^{n-1} \geq \int_\Omega \phi(x,\nabla \tilde{u}) + \frac{\lambda}{2}\int_\Omega |\tilde{u} - I|^2 dx + \int_{\partial\Omega} |\tilde{u} - g| d\mathcal{H}^{n-1}$$

for all $v \in BV \cap L^2(\Omega)$, i.e., $\tilde{u}$ is a pseudosolution of (3.1). □

5. Numerical Methods and Experimental Results. We solve the minimization problem (1.3) numerically using the flow of its associated Euler-Lagrange equation,

$$\frac{\partial u}{\partial t} - \text{div}\,(\phi_{\text{r}}(\text{x}, \text{Du})) + \lambda(\text{u} - \text{I}) = 0, \quad \text{in } \Omega \times [0,T] \quad (5.1)$$

$$\frac{\partial u}{\partial n}(x,t) = 0, \quad \text{on } \partial\Omega \times [0,T] \quad (5.2)$$

$$u(0) = I, \quad \text{in } \Omega \quad (5.3)$$

To approximate (5.1), we use an explicit finite difference scheme. The degenerate diffusion term

$$\text{div}\,(\phi_r(x,\nabla u)) = |\nabla u|^{p(x)-2}\left[(p(x)-1)\Delta u + (2-p(x))|\nabla u|\text{div}\left(\frac{\nabla u}{|\nabla u|}\right) + \nabla p \cdot \nabla u \log|\nabla u|\right]$$

where we chose

$$p(x) = \begin{cases} q(x) \equiv 1 + \frac{1}{1+k|\nabla G_\sigma * I(x)|^2}, & |\nabla u| < \beta \\ 1, & |\nabla u| \geq \beta \end{cases} \quad (5.4)$$

for $k, \sigma > 0$ and G_σ the Gaussian filter, is approximated as follows:

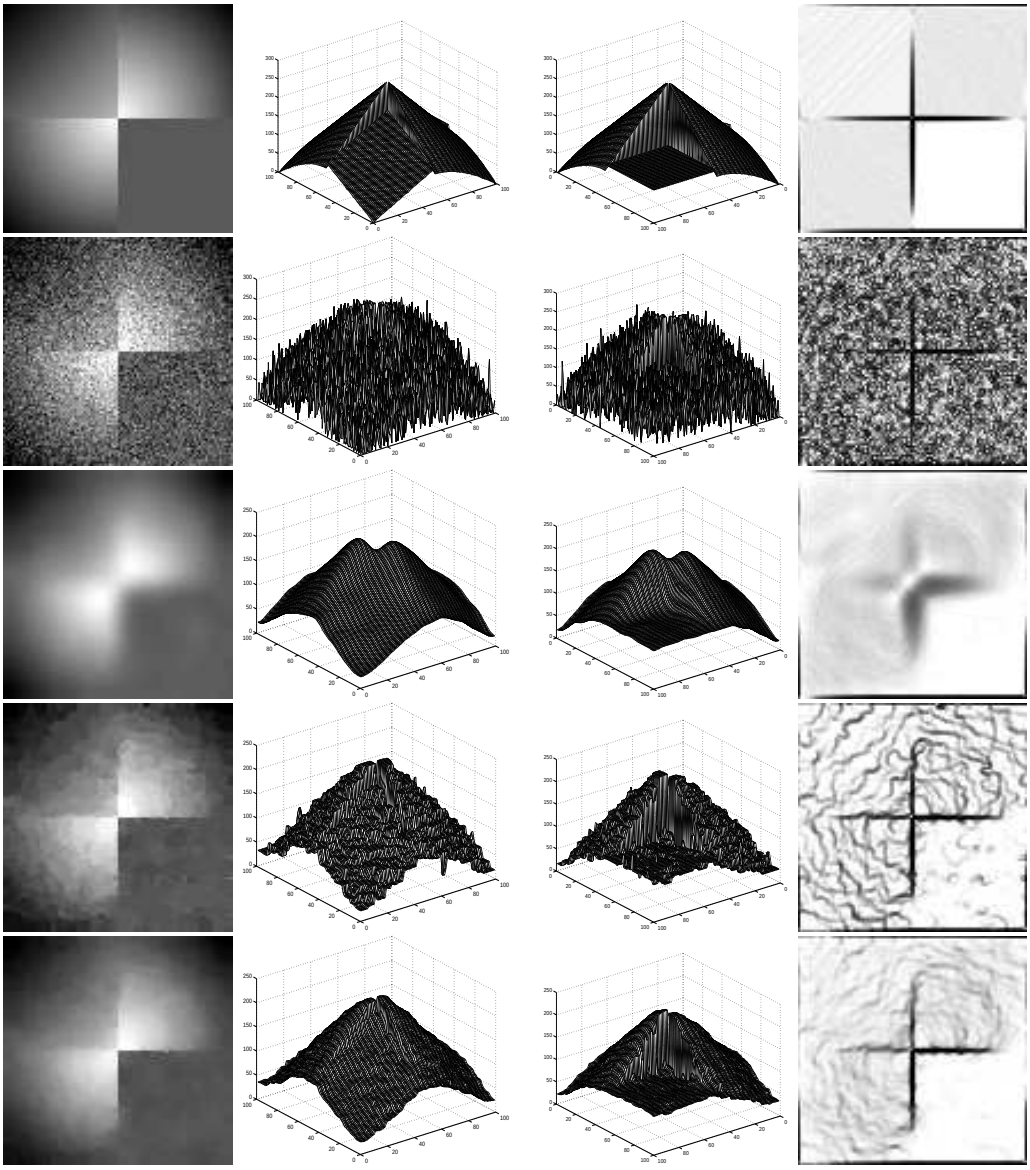

FIG. 5.1. **First Row**: *true image (100×100), surface plot of the image, surface rotated* 180^o*, edge map* (5.6)*;* **Second Row**: *image + noise;* **Third Row**: *reconstruction using isotropic diffusion only (200 iterations):* **Fourth Row**: *reconstruction using TV-based diffusion only (2000 iterations);* **Fifth Row**: *reconstruction using the proposed model (1000 iterations,* β*=30, k=.0075)*

- the coefficient, $|\nabla u|^{p(x)-2}$, is approximated using central differences,
- the isotropic diffusion term, Δu is approximated using central differences,
- the curvature term, $|\nabla u| \text{div}\left(\frac{\nabla u}{|\nabla u|}\right)$ is approximated using the minmod scheme for $\text{div}\left(\frac{\nabla u}{|\nabla u|}\right)$ (see [18]) and central differences for $|\nabla u|$,
- if $|\nabla u| \neq 0$, the hyperbolic term $\nabla p \cdot \nabla u \log |\nabla u|$ is computed using an upwind scheme for $\nabla p \cdot \nabla u$ (see [16]) and central differences for $\log |\nabla u|$. Otherwise, the hyperbolic term is set to zero.

We found that the behavior of (1.3) is innate to the model and variants on this numerical scheme also yield

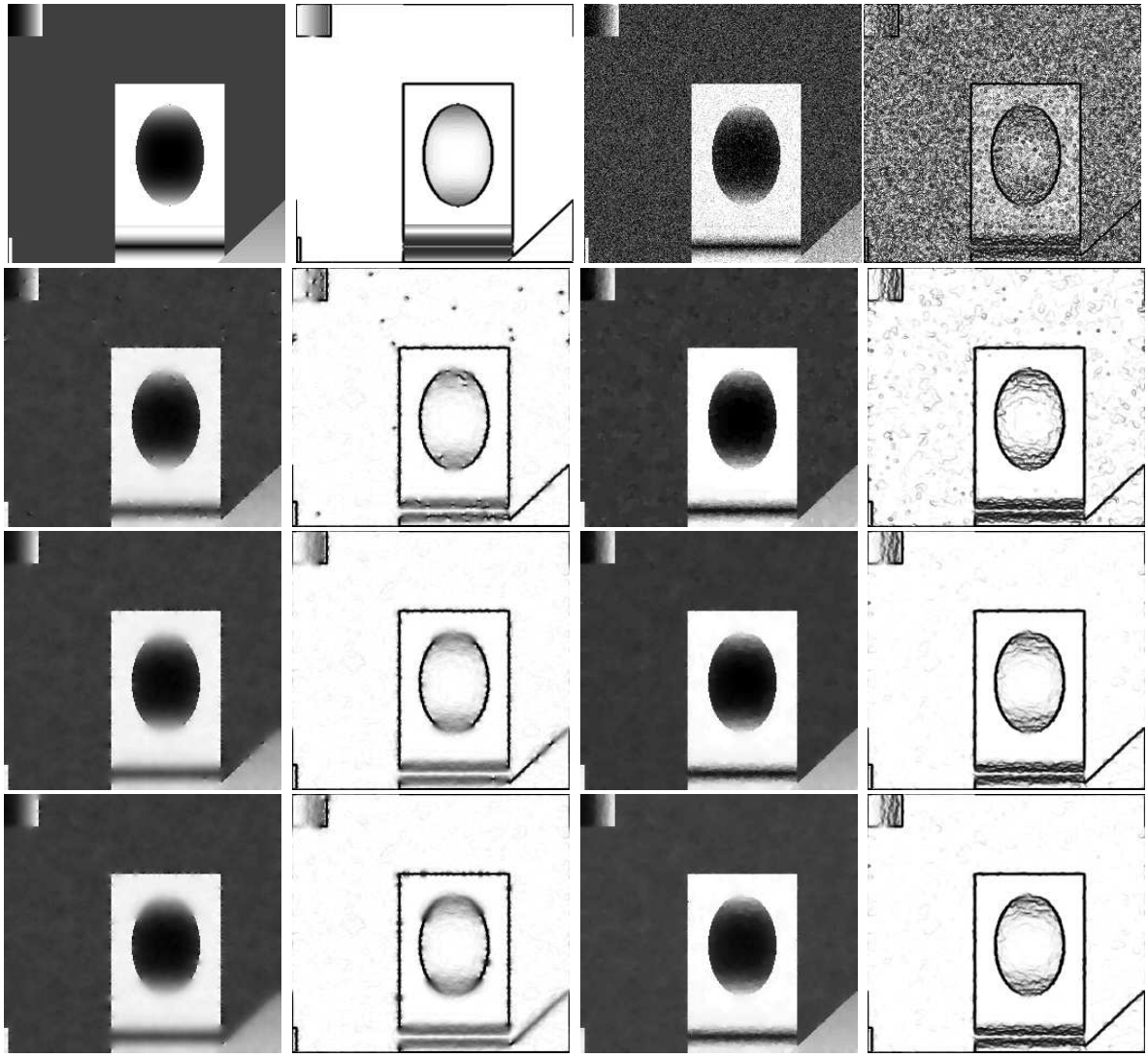

FIG. 5.2. **Top Row**: *original piecewise smooth image (256×256) and edge map* (5.6)*, image + noise and edge map* (5.6)*;* **Bottom Three Rows**: FIRST COLUMN. *reconstructions using* (1.2) *with thresholds* $\beta = 30, 50, 70$ *respectively (1000 iterations);* SECOND COLUMN. *corresponding edge maps* (5.6) THIRD COLUMN. *reconstruction using TV-based diffusion only (2000 iterations) and the proposed model with thresholds* $\beta = 30, 100$ *respectively (1000 iterations);* FOURTH COLUMN. *corresponding edge maps* (5.6) *(all images:* k*=.0075,* λ*=.05,* σ*=.5, timestep=.05)*

very good results.

We compared our model with the flow of the Euler-Lagrange equation associated with (1.2) (modified only by a fidelity term),

$$\frac{\partial u}{\partial t} = (p-1)\Delta u + (2-p)\text{div}\left(\frac{\nabla u}{|\nabla u|}\right) - \lambda(u-I) \quad \text{where} \quad p = \begin{cases} 2, & |\nabla u| < \beta \\ 1, & |\nabla u| \geq \beta \end{cases}. \tag{5.5}$$

An explicit finite difference scheme was used, where central differences were used to implement Δu and the minmod scheme [18] was used to implement div $\left(\frac{\nabla u}{|\nabla u|}\right)$.

All of the images ranged in intensity from 0 to 255. The parameters λ=.05, σ=.5, k = .0075, and time step=.05 consistently yielded optimal results for all of the models we tested here. We compared various thresholds, β, to test both models (1.2) and (1.3)'s sensitivity to this parameter. All of the 'edge maps' in

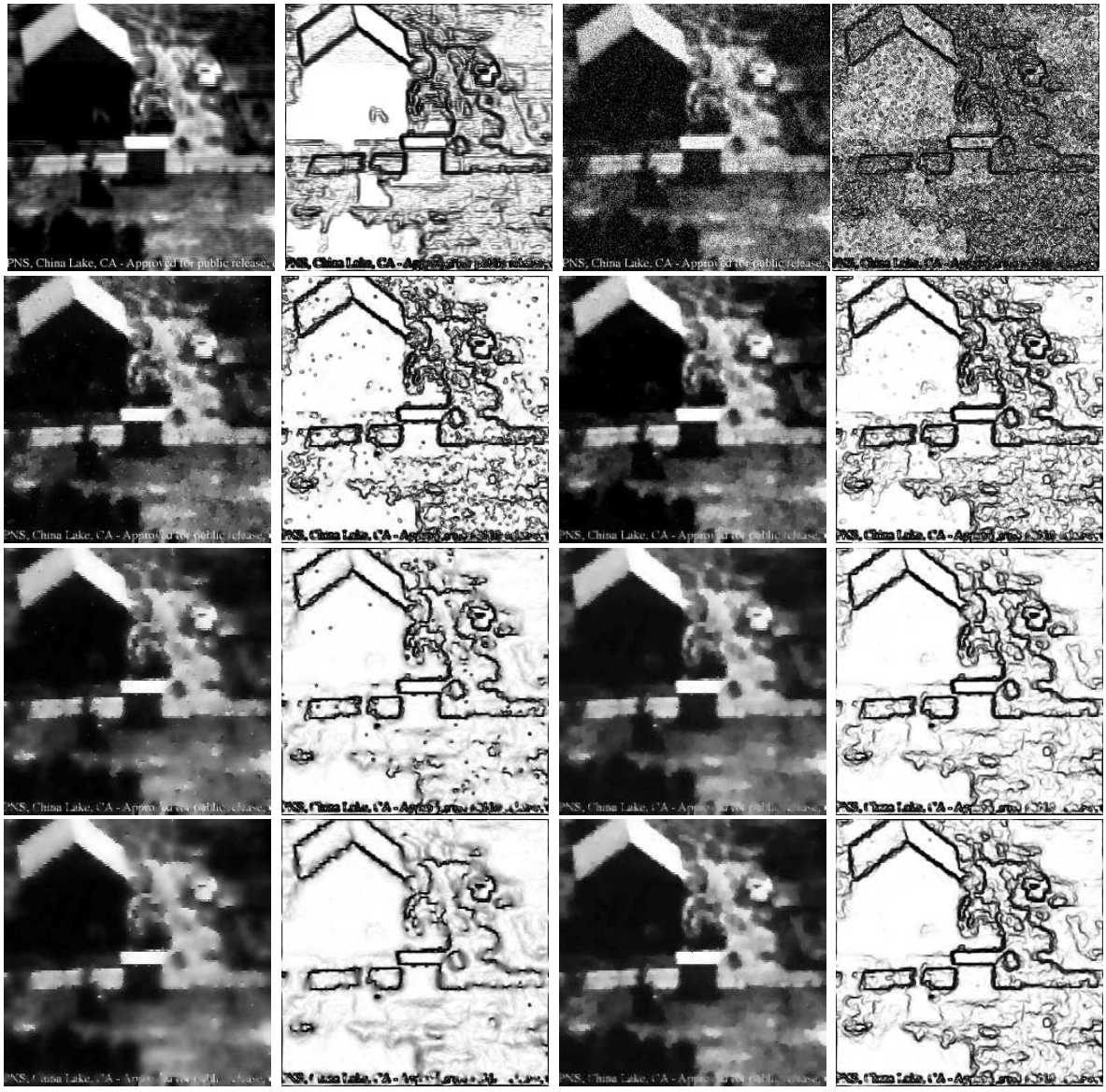

FIG. 5.3. **Top Row**: *radar image (256×256) and edge map* (5.6)*; radar image with Gaussian noise and edge map* (5.6) *with* $k = .0075$*;* **Bottom Three Rows**: FIRST COLUMN. *reconstructions using* (1.2) *with thresholds* $\beta = 10, 20, 30$ *respectively (1000 iterations);* SECOND COLUMN. *corresponding edge maps* (5.6) THIRD COLUMN. *reconstruction using TV-based diffusion only (4000 iterations) and the proposed model with thresholds* $\beta = 30, 100$ *respectively (1000 iterations);* FOURTH COLUMN. *corresponding edge maps* (5.6) *(all images: k=.0075,* λ*=.05,* σ*=.5, timestep=.05)*

the figures were computed using the function

$$\textit{edge map of } u: \quad \frac{1}{1 + k|\nabla G_\sigma * u(x)|^2} \tag{5.6}$$

with $k = .0075$ (the same value of k is also used to compute the exponent $p(x)$ in (5.4)). We found that this value also gave the clearest edge map for each model. The number of iterations were chosen large enough so that the standard deviation between subsequent images was at most .005.

In figure 5.1 we illustrate the proposed model's ability to reconstruct piecewise smooth functions while avoiding the staircasing effect. The first row contains a piecewise smooth function plotted as both an image and a surface, as well as it's edge map (5.6). The surface is viewed from two different orientations; the first

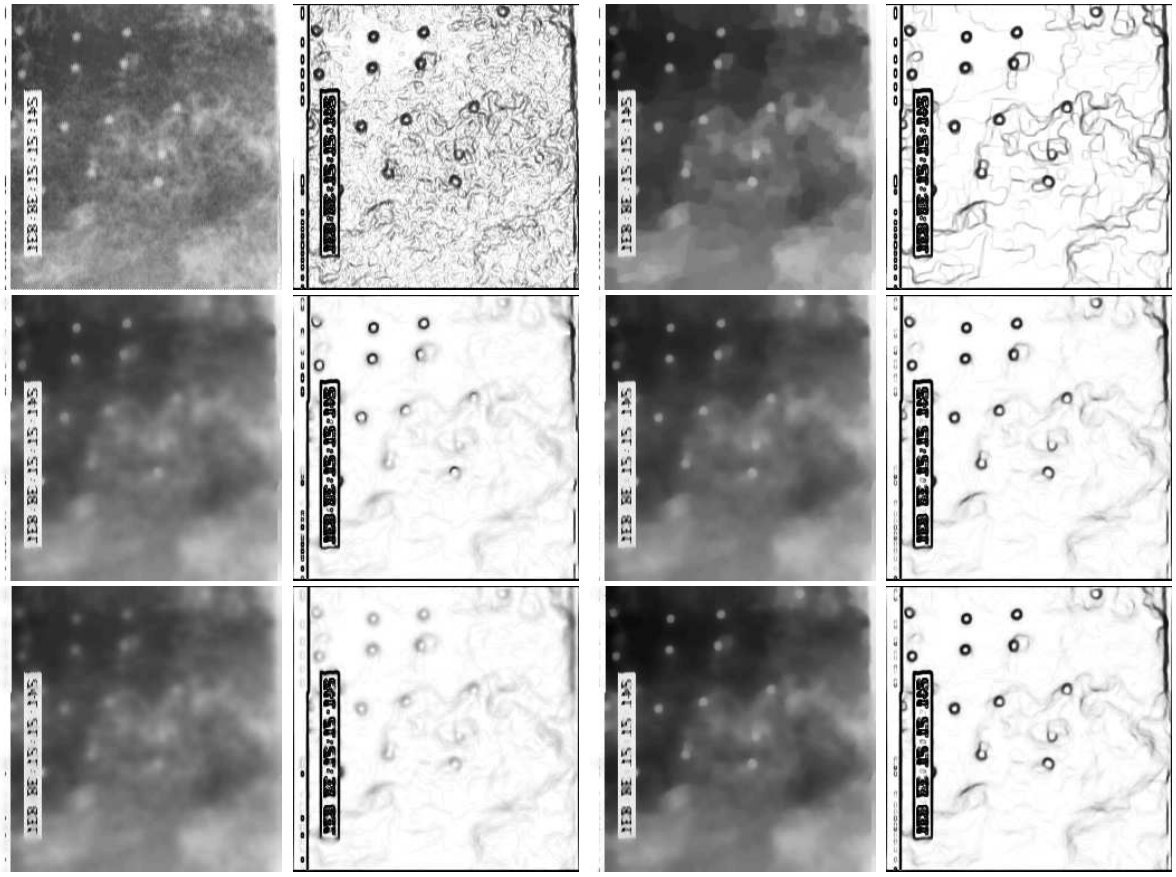

FIG. 5.4. **First Column**: *radar image of land mines (256×256), reconstructions using* (1.2) *with thresholds* $\beta = 10, 20$ *respectively (750 iterations);* **Second Column**: *corresponding edge maps* (5.6)*;* **Third Column**: *reconstruction using TV-based diffusion only (1000 iterations), reconstructions using the proposed model with thresholds* $\beta = 30, 100$ *respectively (750 iterations);* **Fourth Column**: *corresponding edge maps* (5.6)*; (all images: k=.0075, λ=.05, σ=.5, timestep=.05)*

view displays the upper left corner of the image at the origin and the second is the same surface rotated 180^o. The second row contains the same series of images for the image degraded by Gaussian noise with mean zero. The third, fourth, and fifth rows contain reconstructions using isotropic diffusion only ($p \equiv 2$), TV-based diffusion only ($p \equiv 1$), and the proposed model respectively. Isotropic diffusion reconstructs smooth regions, but edges are severely blurred. TV-based diffusion reconstructs sharp edges, but the 'staircasing effect' is clearly present. This in turn creates false edges which could lead to an incorrect segmentation of the image. The proposed model reconstructs sharp edges as effectively as TV-based diffusion *and* recovers smooth regions as effectively as pure isotropic diffusion (in particular, without staircasing).

Figure 5.2 contains a reconstruction of another piecewise smooth image with additive Gaussian noise. Our goal is to once again reconstruct the smooth regions while preserving their boundaries and without introducing false edges. Furthermore, we also wanted to compare the sensitivity of models (1.2) and (1.3) to the threshold, β. The top row shows the original and noisy images with their edge maps (5.6). The bottom three rows contain reconstructions using models (1.2) and (1.3). The first column contains reconstructions using (1.2) with thresholds $\beta = 30, 50$ and 70 respectively and the second column contains their corresponding edge maps (5.6). The third column contains reconstructions using TV-based diffusion only ((1.2) or (1.3) with $\beta = 0$) and the proposed model (1.3) with thresholds $\beta = 30$ and 100 respectively. The last column contains their corresponding edge maps (5.6). TV-based diffusion only ($\beta = 0$), shows clear evidence of staircasing, while the proposed model is relatively insensitive to a broad range of thresholds, β. Although the exact behavior of the diffusion changes slightly at likely edges between $\beta = 30$ and $\beta = 100$, the effect on the resulting image is minimal. On the other hand, model (1.2) demonstrates a large change in behavior

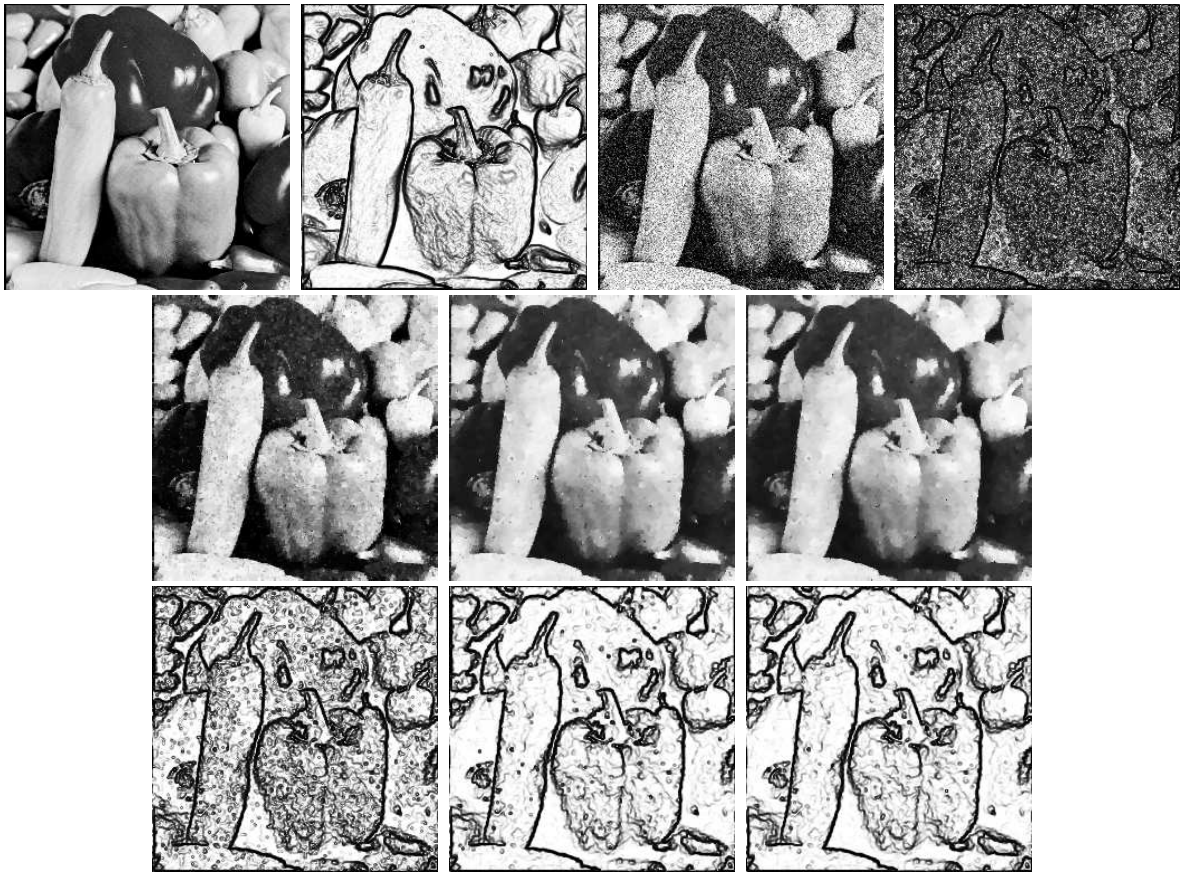

FIG. 5.5. **First Row**: *true image (256×256) and edge map* (5.6)*, true image + noise and edge map* (5.6)*;* **Second Row**: *reconstructions using TV-based diffusion only (2000 iterations) and the proposed model with thresholds* $\beta = 30, 100$ *(1000 iterations,* $k = .0075$*)* **Third Row**: *corresponding edge maps* (5.6) *(all images: k=.0075,* λ*=.05,* σ*=.5, timestep=.05)*

at both noise and edges across the range of thresholds $\beta = 30, 50$ and 70. Similar experiments on the noisy radar images in figures 5.3 and 5.4 yielded very similar results. Note that in figure 5.3, even fine details such as the lettering at the bottom of the image are preserved using the proposed model. In figure 5.4, the proposed model preserves the boundaries of the land mines as effectively as the TV model without enhancing the background noise.

Figure 5.5 provides another successful reconstruction of a piecewise smooth image with additive Gaussian noise. TV-based diffusion alone creates false edges, while the proposed model preserved accurate object boundaries while minimizing the creation of false ones. Tests with $\beta = 30$ and 100 again demonstrate the proposed model's insensitivity to the threshold, β. Figure 5.6 is a similar experiment with an MRI of a heart. The original image is successfully denoised using the proposed model (top row). We then added more noise and as in the previous experiments found that TV alone created false edges while the proposed model generated much fewer false artifacts.

Figure 5.7 contains several more examples in which the noise in each of the images was acquired directly through acquisition, storage, or transmission. The first row contains a diffusion tensor image (DTI) of a brain, the second contains an MRI of a chest cavity, the third contains a transmission electron microscope (TEM) image of aluminum. In all of these images, the goal is to detect 'true' object boundaries without creating any false edges. The proposed model is successful in all of these cases.

Acknowledgments. The authors would like to thank Bernard Mair for the radar images in figures 5.3 and 5.4, Sebastien Barre for the MRI in figure 5.6, and Yijun Liu for the DTI image, Mark Griswold for the MRI, and Katayun Barmak for the TEM image in figure 5.7.

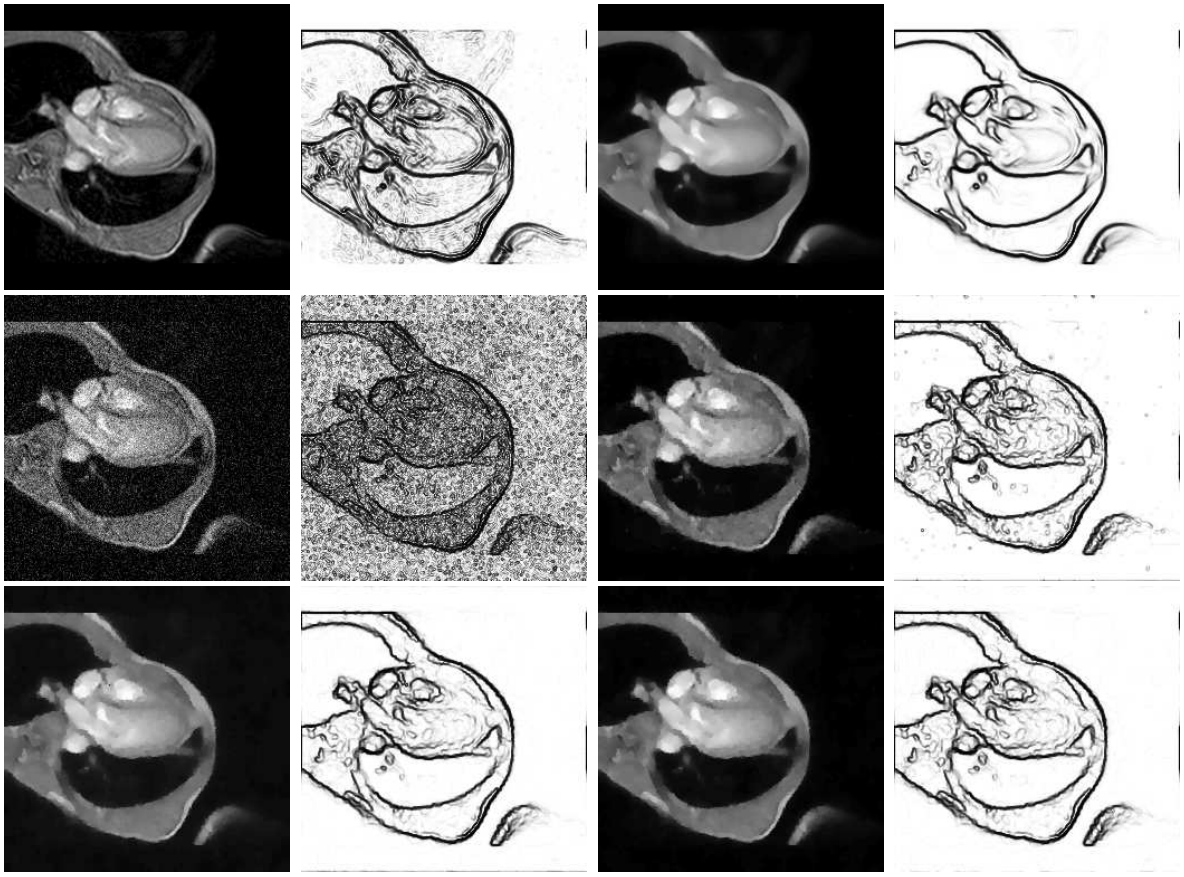

FIG. 5.6. **First Row**: *true image: heart MRI (256×256), corresponding edge map* (5.6)*, reconstruction using the proposed model (threshold* $\beta = 30$*), edge map* (5.6)*;* **Second Row**: *heart MRI + noise, edge map* (5.6)*, reconstruction using TV-based diffusion only, edge map* (5.6)*;* **Third Row**: *reconstruction using the proposed model (threshold* $\beta = 30$*); edge map* (5.6)*, reconstruction using the proposed model (threshold* $\beta = 100$*), edge map* (5.6) *(all images: k=.0075,* λ*=.05,* σ*=.5, timestep=.05)*

REFERENCES

[1] R. ACAR AND C. R. VOGEL, *Analysis of bounded variation penalty methods for ill-posed problems*, Inverse Problems, 10 (1994), pp. 1217–1229.

[2] P. BLOMGREN, T. F. CHAN, P. MULET, AND C. WONG, *Total variation image restoration: Numerical methods and extensions*, Proceedings of the 1997 IEEE International Conference on Image Processing, III (1997), pp. 384–387.

[3] V. CASELLES, J.-M. MOREL, AND C. SBERT, *An axiomatic approach to image interpolation*, IEEE Trans. Image Process., 7 (1998), pp. 376–386.

[4] A. CHAMBOLLE AND P.-L. LIONS, *Image recovery via total variation minimization and related problems*, Numer. Math., 76 (1997), pp. 167–188.

[5] T. F. CHAN, S. H. KANG, AND J. SHEN, *Euler's elastica and curvature-based inpainting*, SIAM J. Appl. Math., 63 (2002), pp. 564–592 (electronic).

[6] T. F. CHAN AND J. SHEN, *Mathematical models for local nontexture inpaintings*, SIAM J. Appl. Math., 62 (2001/02), pp. 1019–1043 (electronic).

[7] Y. M. CHEN AND M. RAO, *Minimization problems and associated flows felated to weighted p energy and total variation*, SIAM J. Math. Anal., 34 (2003), pp. 1084–1104.

[8] D. C. DOBSON AND F. SANTOSA, *Recovery of blocky images from noisy and blurred data*, SIAM J. Appl. Math., 56 (1996), pp. 1181–1198.

[9] L. C. EVANS AND R. F. GARIEPY, *Measure theory and fine properties of functions*, Studies in Advanced Mathematics, CRC Press, Boca Raton, FL, 1992.

[10] E. GIUSTI, *Minimal surfaces and functions of bounded variation*, vol. 80 of Monographs in Mathematics, Birkhäuser Verlag, Basel, 1984.

[11] R. HARDT AND X. ZHOU, *An evolution problem for linear growth functionals*, Comm. Partial Differential Equations, 19 (1994), pp. 1879–1907.

[12] O. A. LADYŽENSKAJA, V. A. SOLONNIKOV, AND N. N. URALCEVA, *Linear and quasilinear equations of parabolic type*,

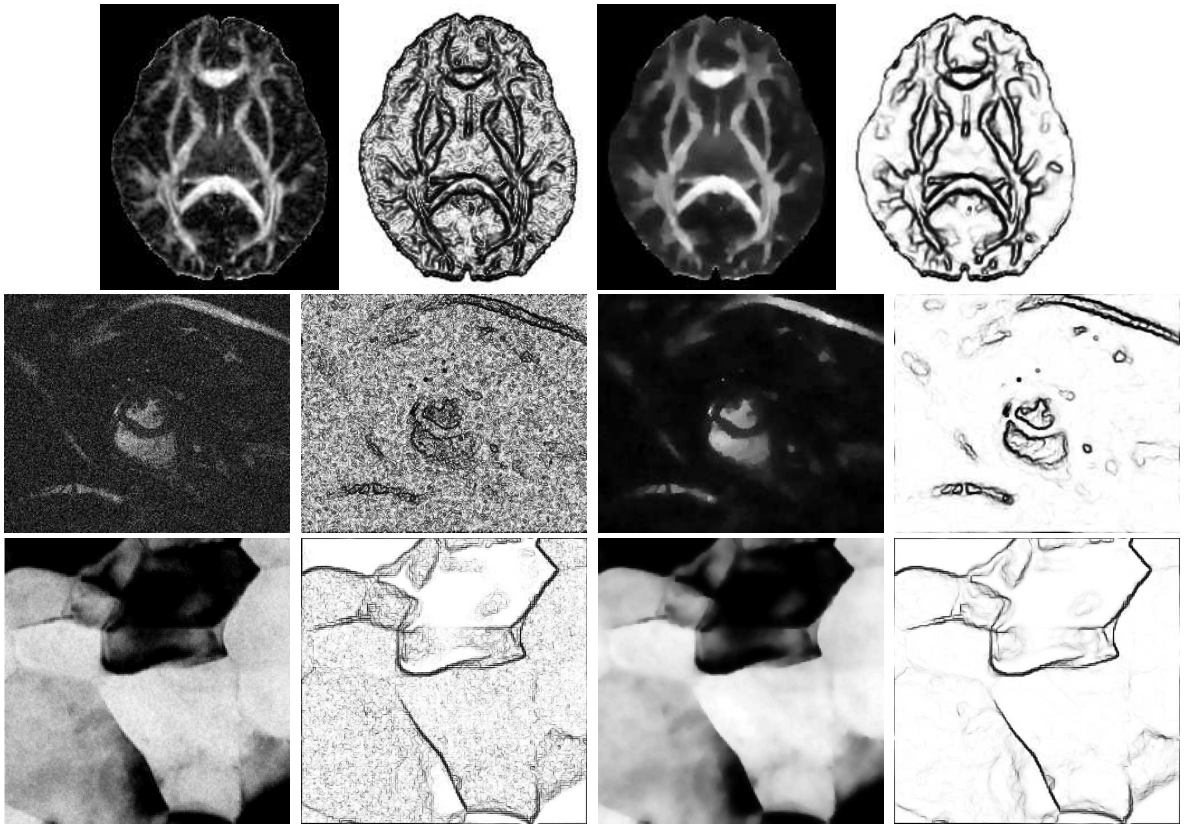

FIG. 5.7. **First Column**: *true images: brain DTI (201×171), chest cavity MRI (209×256), TEM image of aluminum (512×512);* **Second Column**: *corresponding edge maps* (5.6)*;* **Third Column**: *reconstructions using the proposed model (420, 1000, 500, 500 iterations respectively);* **Fourth Column**: *corresponding edge maps* (5.6) *with* $k = .0075$ *(all images: threshold=30, k=.0075,* λ*=.05,* σ*=.5, timestep=.05)*

Translated from the Russian by S. Smith. Translations of Mathematical Monographs, Vol. 23, American Mathematical Society, Providence, R.I., 1967.

[13] A. LICHNEWSKY AND R. TEMAM, *Pseudosolutions of the time-dependent minimal surface problem*, J. Differential Equations, 30 (1978), pp. 340–364.

[14] S. MASNOU AND J. M. MOREL, *Level lines based disocclusion*, IEEE International Conference on Image Processing, Chicago, Illinois (October 4-7, 1998).

[15] M. NIKOLOVA, *Weakly constrained minimization: application to the estimation of images and signals involving constant regions*, J. Math. Imaging Vision, 21 (2004), pp. 155–175.

[16] S. OSHER AND J. A. SETHIAN, *Fronts propagating with curvature-dependent speed: algorithms based on Hamilton-Jacobi formulations*, J. Comput. Phys., 79 (1988), pp. 12–49.

[17] W. RING, *Structural properties of solutions to total variation regularization problems*, M2AN Math. Model. Numer. Anal., 34 (2000), pp. 799–810.

[18] L. RUDIN, S. OSHER, AND E. FATEMI, *Nonlinear total variation based noise removal algorithms*, Physica D, 60 (1992), pp. 259–268.

[19] D. M. STRONG AND T. F. CHAN, *Spatially and scale adaptive total variation based regularization and anisotropic diffusion in image processing*, Technical Report, Univeristy of California, Los Angeles, CA, CAM96-46 (1996).

[20] R. T. WHITAKER AND S. M. PIZER, *A mulit-scale approach to nonuniform diffusion*, Comput. Vis. Graph. Image Process.: Image Understand., 57 (1993), pp. 99–110.

[21] Y.-L. YOU, W. XU, A. TANNENBAUM, AND M. KAVEH, *Behavioral analysis of anisotropic diffusion in image processing*, IEEE Trans. Image Process., 5 (1996), pp. 1539–1553.

[22] X. ZHOU, *An evolution problem for plastic antiplanar shear*, Appl. Math. Optim., 25 (1992), pp. 263–285.